IMPACT OF THE OPERATING CONDITIONS ON THE CORRELATION BETWEEN OH* AND HEAT RELEASE RATE IN HYDROGEN-AIR FLAMES

F. G. Schiavone*, M. Torresi*, S. M. Camporeale*, D. Laera*
f.schiavone11@phd.poliba.it
*Department of Mechanics, Mathematics and Management, Polytechnic University of Bari, Via Orabona 4, Bari 70125, Italy

Abstract
The correlation between the distributions of OH* concentration and heat release rate (HRR) in laminar hydrogen-air flames is investigated, highlighting the differences observed between premixed and diffusion flames and the impact of the operating conditions. First, one-dimensional premixed hydrogen-air flames are considered, showing a characteristic peak shift between OH* and HRR, which is less pronounced or inexistent when considering diffusion hydrogen-air flames. The impact of unburned gas temperature and pressure is studied, showing that an increase of either of the two quantities corresponds to a reduction in the peak shift. Subsequently, the impact of different flame regime is analyzed by considering high-fidelity numerical simulations of a two-dimensional hydrogen-air triple flame, for which diffusion and premixed branches coexist, confirming the observations made for one-dimensional calculations.

Introduction
The distribution of Heat Release Rate (HRR) is fundamental to analyze and predict the structure and dynamics of flames. Nevertheless, HRR direct measurements are impractical, and chemiluminescence (i.e., the spontaneous light emission from excited chemical species in flames) is used as a tracer [1].
A good correlation between CH*, OH* and CO_2* chemiluminescent emissions and HRR is generally observed for steady hydrocarbon flames [1]. For pure methane (CH_4) flames, the peak-to-peak distance between OH* intensity and HRR distributions is smaller than the spatial resolution of most measurements, making OH* an adequate heat release tracer [2]. A correspondence between OH* emission and HRR distributions has been found also for methane-hydrogen blends [3]. For hydrogen (H_2)-air flames, instead, a rather wide distance between the OH* and HRR peaks has been observed, and the correlation between the two quantities has been shown to fail in lean premixed cellular tubular flames [4]. As observed in [5], the fundamental reason leading to these observed differences lies in the interplay between the H-radical pool, the OH* main formation pathways, which are related to the fuel composition, and the heat release process.
In this work, the impact of operating conditions, in terms of unburned gas

temperature, pressure, flame regime and stretch, on such physical-chemical mechanisms and, consequently, on the HRR-OH* correlation is investigated. To this scope, firstly laminar premixed unstrained one-dimensional (1D) H_2-air flames are computed and compared with strained counterflow premixed and diffusion H_2-air flames under various conditions of unburned gas temperature and pressure. Subsequently, the impact of flame regime is further highlighted by considering a H_2-air two-dimensional (2D) triple flame, for which diffusion and premixed branches coexist, to confirm the observations made for 1D flames.

Methodology

One-dimensional flame calculations are performed with Cantera (www.cantera.org), implementing the multi-component transport model and considering the Soret effect, while 2D numerical simulations are carried out with the compressible solver AVBP (www.cerfacs.fr/avbp7x) developed at CERFACS (Toulouse, France). The San Diego (UCSD) [6] scheme is adopted to describe the combustion process.
The OH* formation and consumption process in hydrogen flames relies on the following three elementary reactions [7]:

$$\mathrm{H + O + M \leftrightarrow OH^* + M}, \quad (1)$$
$$\mathrm{OH^* \rightarrow OH} + h\nu, \quad (2)$$
$$\mathrm{OH^* + M \leftrightarrow OH + M}, \quad (3)$$

with $h\nu$ being the energy of the emitted photon. At temperatures below 2800 K, OH* is mainly formed by the recombination reaction (1), while it transfers its excess energy, returning to the ground state, either by emitting light in the radiative decay reaction (2) or by the non-reactive collisional quenching reaction (3) [7].
The sub-scheme by Kathrotia et al. [7] is here adopted to describe OH* formation and consumption. In all cases, the OH* sub-mechanism is simply added to the main reaction scheme as its impact on the ground species' concentrations is negligible [8].

One-dimensional flames

Firstly, freely-propagating, unstretched 1D premixed H_2-air flames at variable unburned mixture temperature T_u, pressure p and equivalence ratio ϕ are compared. The correlation between OH* and HRR distributions is assessed by considering two parameters: the normalized peak-to-peak distance δ and the error estimator Z_{OH^*}. The first one is computed as the distance between the peaks of OH* and HRR distributions, divided by the laminar flame thickness $\delta_L^0 = (T_b - T_u)/\max(dT/dx)$, where T_b is the burned mixture temperature. The second one, instead, quantifies the global quality of the OH*-HRR correlation and has been defined in [9] as:

$$Z_{\mathrm{OH}^*} = \int_x \left(\frac{|\mathrm{HRR}(x)|}{\max(|\mathrm{HRR}(x)|)} - \frac{|c_{\mathrm{OH}^*}(x)|}{\max(|c_{\mathrm{OH}^*}(x)|)} \right)^2, \quad (4)$$

where c_{OH*} is the OH* molar concentration.
As can be observed in Fig. 1, the worst correlation between the two distributions is obtained for stoichiometric values, for which the value of Z_{OH*} is higher. Moreover, this is positively impacted by an increase of pressure, and negatively impacted by an increase of unburned gas temperature. Still, as indicated by the isolines of δ in Fig. 1a, the largest normalized peak-to-peak distance is obtained for lower temperatures.

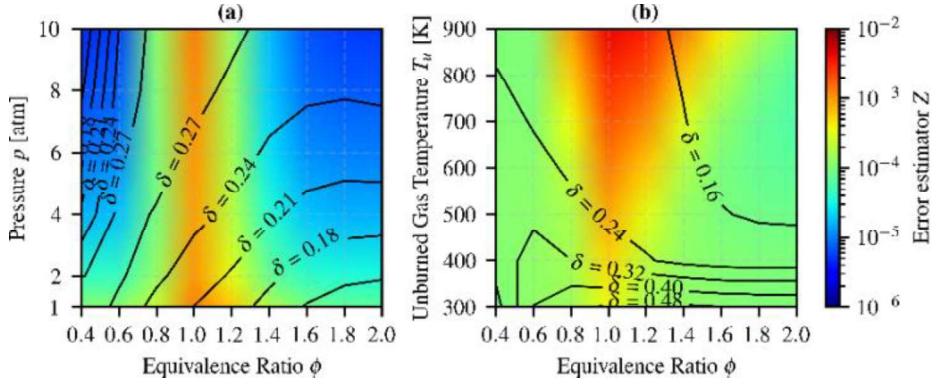

Figure 1. Error estimator Z_{OH*} as a function of ϕ, p and T_u, for T_u = 600 K (a) and p = 1 atm (b). The isolines indicate the corresponding values of δ.

These different trends can be explained by the distributions of OH* concentration and HRR shown in Fig. 2 for stoichiometric flames at three operating points: T_u = 300 K and p = 1 atm (a), T_u = 600 K and p = 1 atm (b), T_u = 600 K and p = 10 atm (c). The computed values of Z are, respectively, 3.53×10^{-4}, 1.26×10^{-3} and 1.25×10^{-3}.

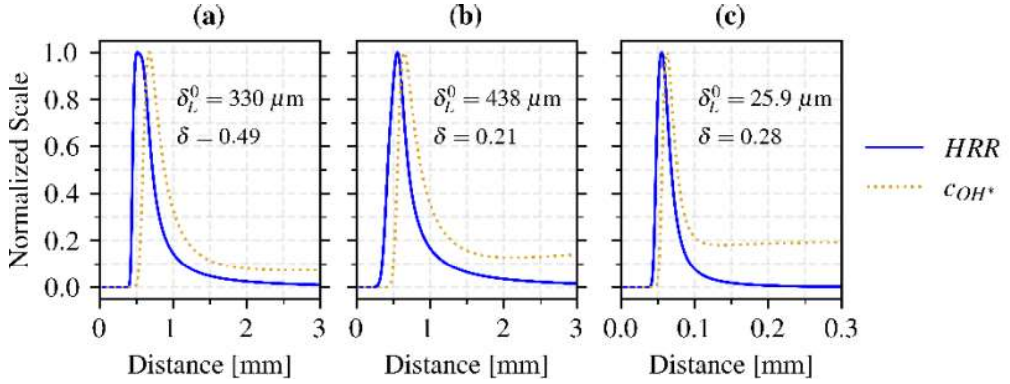

Figure 2. Normalized distributions of HRR and OH* concentration for unstrained premixed flames at ϕ = 1 and T_u = 300 K and p = 1 atm (a), T_u = 600 K and p = 1 atm (b), T_u = 600 K and p = 10 atm (c).

Even though case (a) presents the largest value of δ, the value of Z_{OH*} is the lowest (see Fig. 1a), since the two distributions have the two most similar shapes, mostly due to the reduced equilibrium OH* concentration when compared to the peak one. On the other hand, when increasing T_u and p, the equilibrium OH* concentration increases. Indeed, as the flame temperature increases, OH* production is favored in the post-flame region. The combination of these effects causes a reduction in the

likelihood of the two distributions, with a consequent increase of the value of Z_{OH^*}, even though the value of δ is lower, being the two peaks closer. Consequently, the sole Z_{OH^*} is not sufficient to characterize the correlation between OH* and HRR for H_2-air flames, as it gives a global evaluation of the quality of the correlation, but not an insight into the actual shape and position of the two distributions. As for the impact of operating conditions, it can be observed that, at atmospheric pressure, the peak shift is more accentuated, and is comparable between cases (a) and (b) in terms of physical distance. The different values of δ are in this case due to the increase of flame thickness for higher values of T_u. On the other hand, when pressure increases, the actual physical distance between the peaks is significantly smaller, even though it is more impacting in terms of δ with respect to case (b) due to the reduction of flame thickness given by the pressure increase.

To investigate the impact of flame stretch and regime on the peak shift, 1D stoichiometric twin premixed counterflow flames, for which two jets of premixed fresh gases are opposed to each other, and 1D counterflow diffusion flames, for which a jet of fuel is opposed to a jet of oxidizer, are considered. Flame strain is evaluated as $a = (|u_1| + |u_2|)/d$, where u_1 and u_2 are the inlet velocities of the jets, and d is their distance. The distributions of normalized OH* and HRR are shown, with the corresponding values of δ, in Fig. 3 for $a = 1.0\times10^4$ s^{-1}, a value of strain sufficiently high to highlight stretch effects and, at the same time, not too close to the extinction strain rate, which is approximately 1.8×10^4 s^{-1} for case (a) [5].

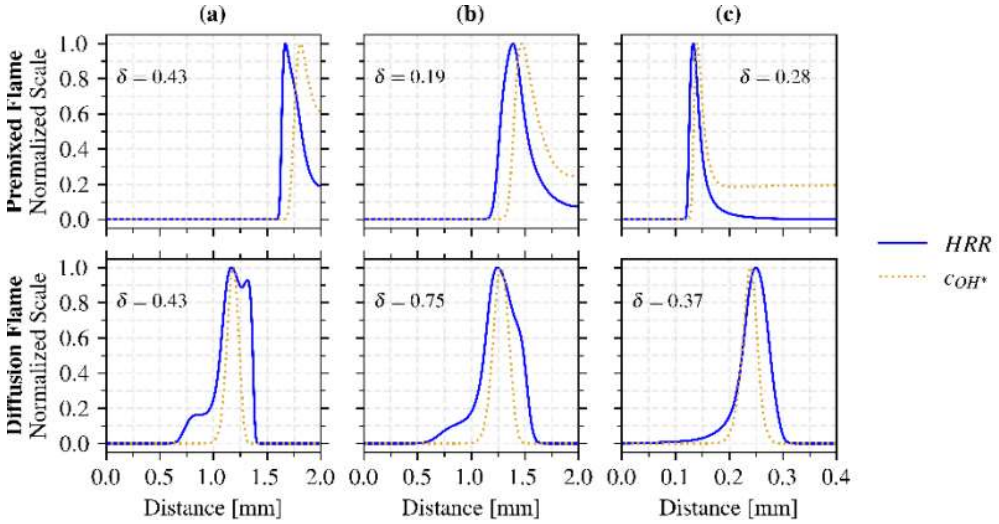

Figure 3. Normalized distributions of HRR and OH* concentration for premixed (top) and diffusion (bottom) counterflow flames at $a = 1.0\times10^4$ s^{-1} and $T_u = 300$ K and $p = 1$ atm (a), $T_u = 600$ K and $p = 1$ atm (b), $T_u = 600$ K and $p = 10$ atm (c).

For the premixed cases, stretch has a limited impact on the peak shift, which remains of the same order of magnitude as in the unstrained case.

On the other hand, the diffusion flames, at least for cases (a) and (b) at atmospheric pressure, show a sensible reduction of the peak shift. Due to the significantly smaller size of the flame front, no appreciable reduction in the peak shift can be found in

case (c). Nevertheless, an agreement in the shape of the distributions, which lacks in the corresponding premixed case, can be observed, sustaining the adequacy of OH* concentration as HRR marker in diffusion H_2-air flames.

Triple flame

The impact of flame regime on the OH*-HRR correlation is further analyzed by considering a 2D triple flame at T_u = 300 K and p = 1 atm, for which three zones can be identified: a lean premixed branch, a rich premixed branch, and a diffusion branch. The HRR fields are shown in Fig. 4 for the premixed (a) and diffusion (b) zones, together with isolines (white) of OH* concentration and the stoichiometric line (black). A sensible axial shift can be observed between the HRR and OH* peaks, with the former being located further down, in the rich premixed zone, while the latter is above, close to the stoichiometric line and in proximity of the triple point. On the other hand, the OH* distribution shows to be better correlated to the HRR one, with the two peaks located in the same region and the OH* field able to capture with sufficient adequacy the HRR variation in the whole zone.

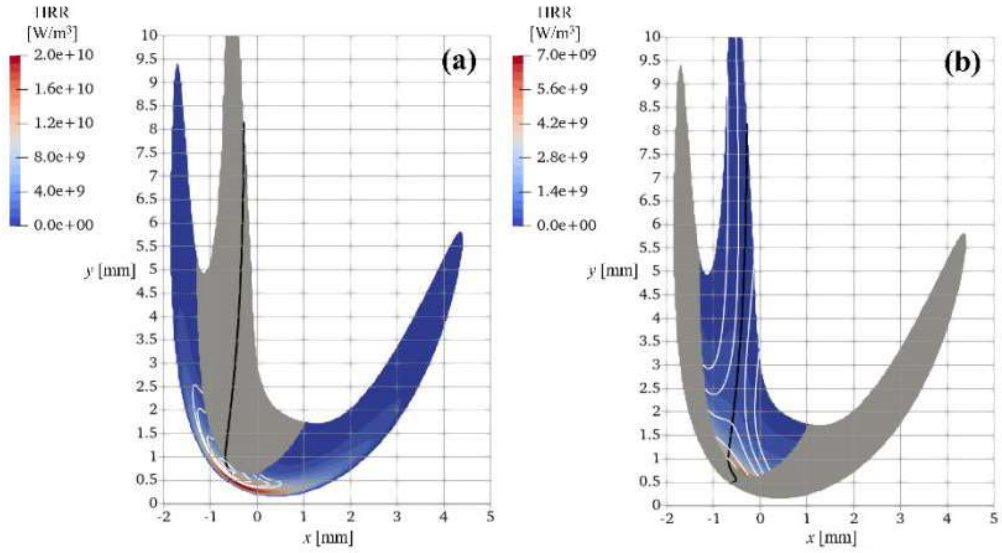

Figure 4. HRR distributions for a triple flame at T_u = 300 K and p = 1 atm in the premixed (a) and diffusion (b) zones, isolines (white) at 90%, 50%, 20%, 10% and 5% of maximum OH* concentration in each zone, and stoichiometric line (black).

Conclusion

In this work, the correlation between heat release rate (HRR) and OH* concentration in hydrogen-air flames has been investigated, focusing on the impact of operating conditions, in terms of unburned gas temperature, pressure, flame regime and stretch. By performing 1D calculations, it has been observed that OH* poorly correlates with HRR for premixed flames, with a sensible shift between the peaks of the two distributions, especially for low pressures, at all equivalence ratios. A similar behavior has been observed also for stretched premixed flames, while a significant improvement in terms of peak shift reduction has been found for diffusion flames.

This behavior has been confirmed also in a 2D triple flame, sustaining the adequacy of OH* as HRR marker for hydrogen-air diffusion flames only, while an error is to be considered for premixed cases. This is especially true for low-pressure cases, which are typical of OH* chemiluminescence experimental measurements.

Acknowledgments
The authors would like to acknowledge CERFACS for the grant to use the AVBP code. High-Performance Computing resources from CINECA (ISCRA-C Project INTONATE), MeluXina/LuxProvide and EuroHPC JU (Project PROMETH2EUS), and CRESCO/ENEAGRID are acknowledged. This work was supported by the Italian Ministry of University and Research under the National Recovery and Resilience Plan funded by the European Union - NextGenerationEU (Project: CNMS named MOST, CUP: D93C22000410001, Spoke 14 "Hydrogen and 11 New Fuels").

References
[1] Lauer, M., Sattelmayer, T., "On the adequacy of chemiluminescence as a measure for heat release in turbulent flames with mixture gradients", *J. Eng. Gas Turbines Power* 132(6): 061502 (2010).
[2] Panoutsos, C. S., Hardalupas, Y., Taylor, A. M. K. P., "Numerical evaluation of equivalence ratio measurement using OH* and CH* chemiluminescence in premixed and non-premixed methane–air flames", *Combust. Flame* 156(2): 273-291 (2009).
[3] Reyes, M., Tinaut, F. V., Giménez, B., Pastor, J. V., "Effect of hydrogen addition on the OH* and CH* chemiluminescence emissions of premixed combustion of methane-air mixtures", *Int. J. Hydrogen Energy* 43(42): 19778-19791 (2018).
[4] Marshall, G. J., Pitz, R. W., "Evaluation of heat release indicators in lean premixed H2/Air cellular tubular flames", *Proc. Combust. Inst.* 37(2): 2029-2036 (2019).
[5] Schiavone, F. G., Aniello, A., Riber, E., Schuller, T., Laera, D., "On the adequacy of OH* as heat release marker for hydrogen-air flames", *Proc. Combust. Inst.*, Manuscript accepted for presentation (2024).
[6] Saxena, P., Williams, F. A., "Testing a small detailed chemical-kinetic mechanism for the combustion of hydrogen and carbon monoxide", *Combust. Flame* 145(1-2): 316-323 (2006).
[7] Kathrotia, T., Fikri, M., Bozkurt, M., Hartmann, M., Riedel, U., Schulz, C., "Study of the H+O+M reaction forming OH*: Kinetics of OH* chemiluminescence in hydrogen combustion systems", *Combust. Flame* 157(7): 1261-1273 (2010).
[8] Graña-Otero, J., Mahmoudi, S. "Excited OH kinetics and distribution in H2 premixed flames", *Fuel* 255: 115750 (2019).
[9] Nikolaou, Z. M., Swaminathan, N., "Heat release rate markers for premixed combustion", *Combust. Flame* 161(12): 3073-3084 (2014).